

Electronic Supplementary Information (ESI)

# **Super-tough conducting carbon nanotube/ultrahigh-molecular-weight polyethylene composites with segregated and double-percolated structure**

**Huan Pang,<sup>a</sup> Ding-Xiang Yan,<sup>a</sup> Yu Bao,<sup>a</sup> Jin-Bing Chen,<sup>a</sup> Chen Chen,<sup>b</sup> and Zhong-Ming Li<sup>\*a</sup>**

<sup>a</sup> College of Polymer Science and Engineering, State Key Laboratory of Polymer Materials Engineering, Sichuan University, Chengdu, 610065, Sichuan, People's Republic of China. Fax: +86-28-85401988; Tel: +86-28-85406866; E-mail: [zml@scu.edu.cn](mailto:zml@scu.edu.cn)

<sup>b</sup> Analytical and Testing Center, Sichuan University, Chengdu, 610065, Sichuan, People's Republic of China.

### Morphological images of CNTs

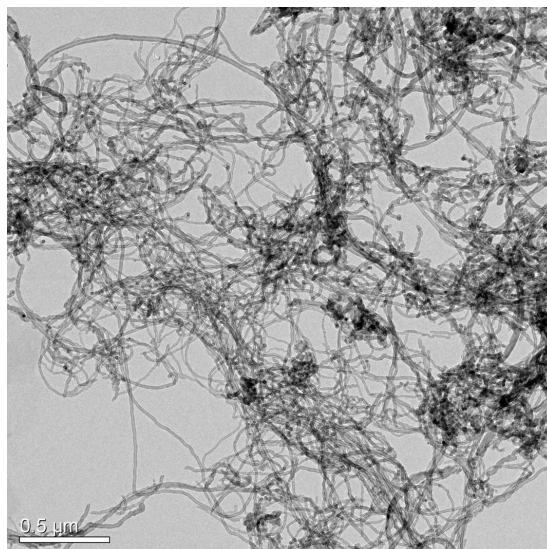


**Fig. S11** Transmission electron microscopy (TEM) image of CNTs.

Observed from TEM image of CNTs (Fig. S11), immediate evidence to prove the existence of CNTs with a large aspect ratio (20–40 nm and length 10–20  $\mu\text{m}$ ) can be offered. Due to the large interface surface and intensive Van der Waals force, CNTs always manifest the agglomerate state as shown in Fig. S11.

### Particle size of the polymer granules

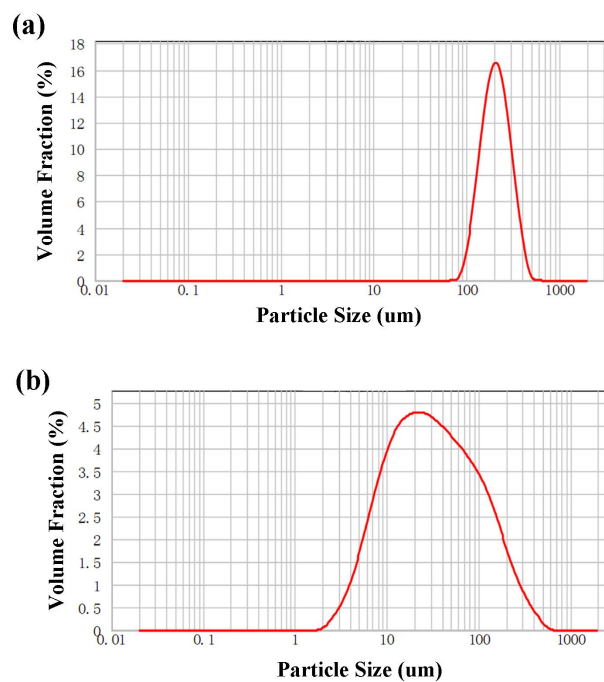


**Fig. S12** Particle size of UHMWPE (a) and CNT/HDPE (b) granules.

Fig. S12 clearly displays the particle size distribution of UHMWPE and CNT/HDPE granules. The particle size of UHMWPE powders is  $\sim 200 \mu\text{m}$  with a mono-disperse and that of CNT/HDPE is  $\sim 50 \mu\text{m}$  with a poly-disperse, which may be ascribed to non-uniformity resulting from the specific high-speed mechanical crushing processing method. These results are indicative of that the particle size of CNT/HDPE powders is small enough to cover around the UHMWPE granules.

### Morphology of the nascent conductive powders

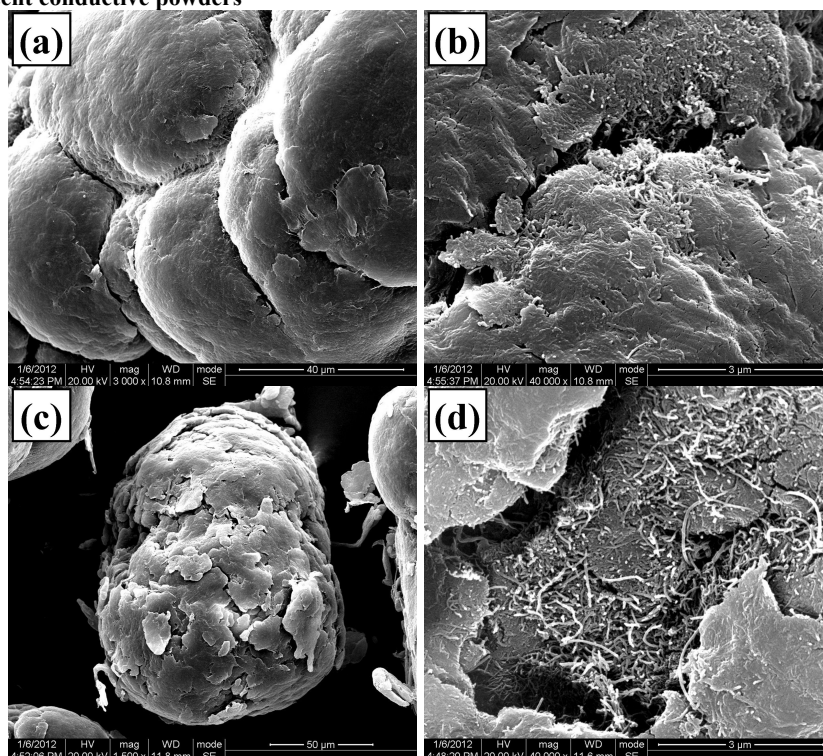


**Fig. S13** SEM photographs of the surface morphology of the nascent UHMWPE particles with a layer of CNTs (a) and CNT/HDPE particles (c) before compression molding, and CNTs (b) and CNT/HDPE granules (d) adsorbed on the surface of UHMWPE particles.

Fig. S13a exhibits the surfaces of the nascent UHMWPE powders which are partly connected by CNTs threads. Although the CNT agglomerates are non-uniformly dispersed on the surfaces of UHMWPE particles (Fig. S13b), CNT conductive networks are still formed. This is a little different from our previous work in which CNTs were more uniformly distributed on the surfaces of UHMWPE by alcohol-assisted ultrasound dispersion.<sup>1</sup> In Fig. S3c, the UHMWPE granules are partly coated with CNT/HDPE particles, and the completed CNT conductive network is obvious in the CNT/HDPE granules (Fig. S13d).

### Thickness of conductive pathway

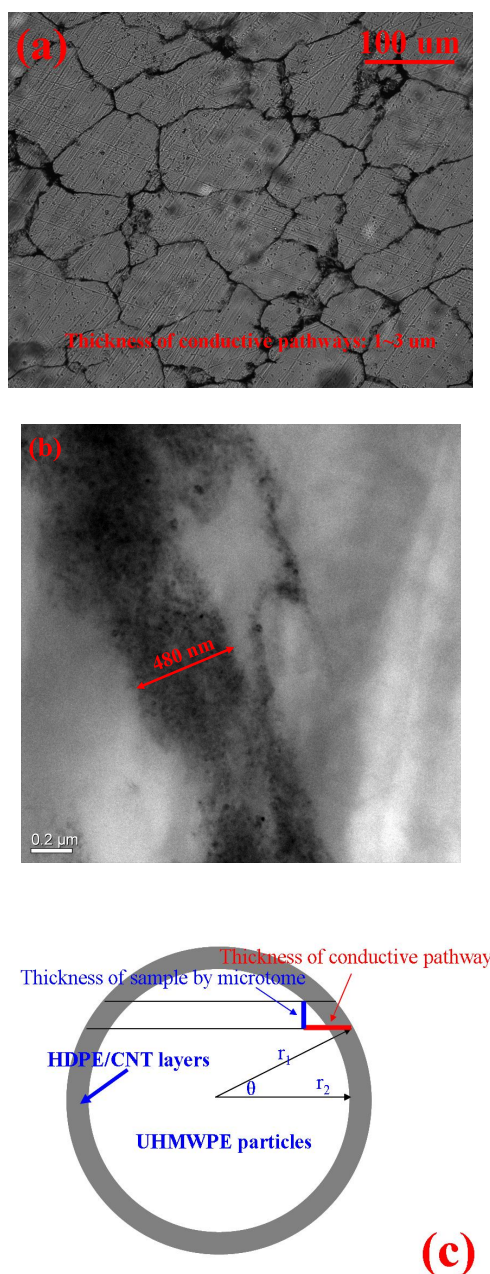


**Fig. S14** Optical images of CNT/HDPE/UHMWPE (a) and TEM micrographs of CNT/HDPE/UHMWPE (b). An illustration for the relationship between thickness of the samples and conductive pathways (c).

Suppose that the shape of UHMWPE particles does not change greatly during the hot compaction (Fig. S14).  $r_2$  and  $r_1$  are respectively defined as the radius of the UHMWPE particle and the UHMWPE particle covered with conducting fillers. So the thickness of the CNT network can be presented by  $h$  which is equal to  $r_1 - r_2$ . Consequently, the boundary thickness can be calculated, namely, the theoretical thickness of the CNT conductive network is only about 50 and 950 nm for segregated CNT/UHMWPE and segregated and double-percolated CNT/HDPE/UHMWPE CPCs, respectively, when the weight fraction of CNT is 0.3%.

As displayed in Fig. S14a and b, it is clear to find that the theoretical thickness of conductive pathway is different from those measure in OM image (1~3  $\mu\text{m}$ ) and TEM image (~480 nm). This phenomenon can be ascribed to two factors. According to the classical stereological relationship (Fig. S14c), the thickness of conductive network is increasing with the thickness of samples by microtome. The thickness of specimens for OM (~10  $\mu\text{m}$ ) is much larger than that of TEM bars (~80 nm). In addition, due to the magnified limitation of OM observation, the pullout of CNT agglomerations may also result in the increasing thickness of the conductive pathways.

### Electrical properties of composites

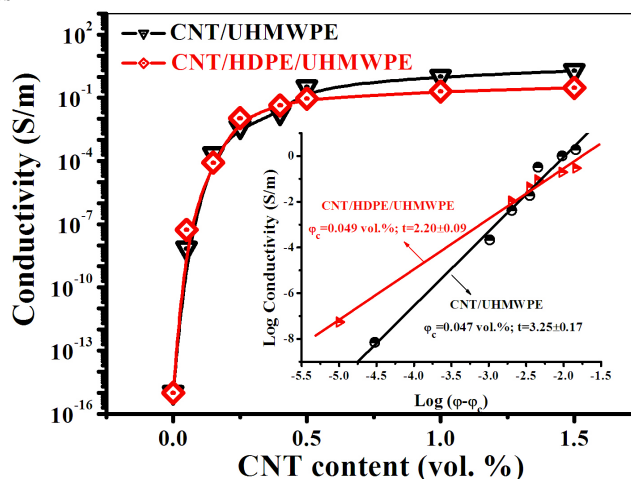


**Fig. S15** Electrical conductivity as a function of CNT content for the CNT/UHMWPE and CNT/HDPE/UHMWPE composites.

Fig. S15 shows the conductivity of the composite as a function of the CNT content. When the CNT content is about 0.047 and 0.049 vol. %, the percolation threshold, at which the conductivity increases sharply, is clearly observed for the segregated CNT/UHMWPE and segregated and double-percolated CNT/HDPE/UHMWPE composites, respectively. As expected, the tailored segregated and double-percolated structure generates a very low percolation threshold of below 0.05 vol. % for the CNT-filled polymer composite, which is lower than the percolation threshold of 0.072 vol. % for the segregated CNT/UHMWPE composites by alcohol-assisted dispersion under ultrasonication to disperse CNTs in our previous work.<sup>1</sup> As shown in Fig. S15, the composite with 1.0 vol. % CNT possesses a conductivity of  $\sim 10^{-1}$  S/m (CNT/HDPE/UHMWPE) and  $\sim 1$  S/m (CNT/UHMWPE), which is sufficient for many electrical applications.

The conductivity of the composites can be further rationalized in terms of modified classical percolation theory,  $\sigma = \sigma_0(\varphi - \varphi_c)^t$ , where  $\sigma$  represents the conductivity of the composite,  $\varphi$  is the volume fraction of the filler,  $\varphi_c$  is the volume percolation concentration, and  $t$  is the critical exponent. For a single percolation system, the critical exponent depends only on the dimensionality of the composites and follows a power-law dependence of approximately 2 (1.6–2) in a three dimensional, and 1–1.3 in a two-dimensional system. Using the data of Fig. S15, it is estimated to be 3.25 for CNT/UHMWPE and 2.20 for CNT/HDPE/UHMWPE system, which implies the presence of an approximate three-dimensional conductive network. This result is also different from our previous work, where  $t$  was estimated about 1.13 indicating an ideal two-dimensional conductive network.<sup>1</sup> For CNTs, due to their large surface energy, they cannot be dispersed uniformly only by high-speed mechanical mixing, but can form conductive networks, even at the extremely low filler loading such as below 0.1 vol. %.<sup>2,3</sup> Although the alcohol-assisted dispersion under ultrasonication can avoid the agglomeration of CNTs, the formation of CNTs may not be easily constructed than simply high-speed mechanical mixing. Compared with the heterogeneous distribution of pure CNTs, the CNT/HDPE composites, to some extent, can avoid the further aggregation of CNTs and disperse CNTs more uniformly around UHMWPE particles, resulting in an ordered conducting polymer layers and depressing the value of  $t$ .

### Morphology of impact fractured surface

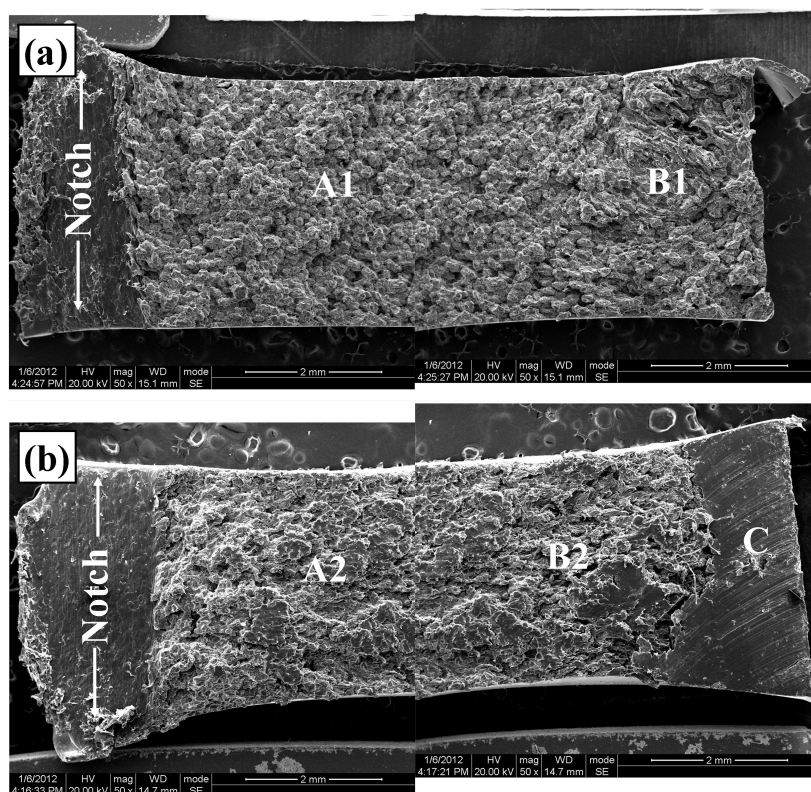


**Fig. SI6** Low magnification SEM micrographs of impact fractured surfaces for the CNT/UHMWPE (a) and CNT/HDPE/UHMWPE (b) composites. The capital letters in the pictures, A1 and A2, crack growth region; B1 and B2, crack blunting region.

The impact fractured surface was also observed in Fig. SI6, in order to elucidate the energy absorption mechanism on the toughness of the semi-rigid segregated conducting composites. Fig. SI6 presents the SEM fractographs of the impact fractured CNT/UHMWPE and CNT/HDPE/UHMWPE composites, respectively. Apparently, the fracture surfaces are composed of two distinct zones: crack growth region (around A) and crack blunting zone (around B). For simplicity these two zones will be referred to as A1, A2 and B1, B2 zones for the CNT/UHMWPE and CNT/HDPE/UHMWPE composites, respectively, hereafter. The CNT/HDPE/UHMWPE bar was not completely fractured by impact (Fig. SI6b). Zone C was made by cutting with a razor, which was reasonably assigned to the crack blunting zone (Zone B2).

The breakdown of the craze initiation might lead to the propagation of a crack (Zone A1 and A2). For the CNT/UHMWPE composite in Fig. SI6a, Zone A1 shows a brittle-like fracture and UHMWPE granules are all pulled out from the matrix, demonstrating a poor adhesive interaction between UHMWPE particles. On the contrary, for the crack growth region of the CNT/HDPE/UHMWPE bar, shown in Fig. SI6b, it can be found that there are regions that underwent somewhat ductile deformation in Zone A2. Different from the smooth fracture surfaces of the CNT/UHMWPE composite, the impact fracture morphology of CNT/HDPE/UHMWPE exhibits rougher and plastic-deformed fracture surfaces, suggestive of the effective adhesive effect of the CNT/HDPE layers coating around the surfaces of UHMWPE particles. Additionally, there are enormous HDPE filaments (Fig. SI6b), also reflecting a high resistance to crack growth for CNT/HDPE/UHMWPE. The crack blunting region (Zone B1 and B2) is at the end of the fracture surface. The rather irregular deformed UHMWPE particles imply the large plastic deformation in this region. In Fig. SI6a, the crack blunting region of the CNT/UHMWPE composites manifests a ductile deformation to a certain extent. For the impact fracture morphology of CNT/HDPE/UHMWPE in crack blunting region, both CNT/HDPE and UHMWPE matrix experienced a considerable plastic deformation, resulting in the formation of fibrillation (Fig. SI6b). These interesting observations further confirm the stronger adhesive interaction between UHMWPE granules for the CNT/HDPE/UHMWPE composites than that of the CNT/UHMWPE one. Moreover, the area of Zone B2 and C is roughly two times larger than that of Zone B1. This larger area of crack blunting region might be a reason of the larger impact strength of the CNT/HDPE/UHMWPE bar.

### Notes and references

- 1 J. F. Gao, Z. M. Li, Q. J. Meng and Q. Yang, *Mater. Lett.*, 2008, **62**, 3530-3532.
- 2 Q. M. Liu, J. C. Tu, X. Wang, W. X. Yu, W. T. Zheng and Z. Zhao, *Carbon*, 2012, **50**, 339-341.
- 3 J. C. Grunlan, A. R. Mehrabi, M. V. Bannon and J. L. Bahr, *Adv. Mater.*, 2004, **16**, 150-153.